Oxidative Degradation of Tannic Acid in Aqueous Solution by UV/S$_2$O$_8{}^{2-}$ and UV/H$_2$O$_2$/Fe^{2+} Processes: A Comparative Study

Sondos Dbira [1], Nasr Bensalah [2],* , Moustafa M. Zagho [3], Massouda Ennahaoui [1] and Ahmed Bedoui [1]

[1] Department of Chemistry, Faculty of Sciences of Gabes, University of Gabes, Gabes 6072, Tunisia; sondos.dbira@gmail.com (S.D.); msdennahoui@gmail.com (M.E.); ahmed.bedouifsg@yahoo.com (A.B.)

[2] Department of Chemistry and Earth Sciences, College of Arts and Sciences, Qatar University, Doha 2713, Qatar

[3] Materials Science and Technology Program, College of Arts and Sciences, Qatar University, Doha 2713, Qatar; mmsalah@qu.edu.qa

* Correspondence: nasr.bensalah@qu.edu.qa; Tel.: +974-4403-6540

check for updates

Abstract: Tannic acid (TA) is a major pollutant present in the wastewater generated from vegetable tanneries process and food processing. This work studied TA degradation by two advanced oxidation processes (APOs): UV irradiation at the wavelength of 254 nm in the presence of hydrogen peroxide (H$_2$O$_2$) and ferrous iron (photo-Fenton) and in the presence of potassium persulfate. The influence of certain experimental parameters such as K$_2$S$_2$O$_8$, H$_2$O$_2$, Fe^{2+}, and TA concentrations, initial pH and temperature was evaluated in order to obtain the highest efficiency in terms of aromatics (decay in UV absorbance at 276 nm) and TOC removals. Chemical oxidation of TA (0.1 mM) by UV/persulfate achieved 96.32% of aromatics removal and 54.41% of TOC removal under optimized conditions of pH = 9 and 53.10 mM of K$_2$S$_2$O$_8$ after 60 min. The treatment of TA by photo-Fenton process successfully led to almost complete aromatics removal (99.32%) and high TOC removal (94.27%) from aqueous solutions containing 0.1 mM of TA at natural pH = 3 using 29.4 mM of H$_2$O$_2$ and 0.18 mM of Fe^{2+} at 25 °C after 120 min. More efficient degradation of TA by photo-Fenton process than UV/persulfate was obtained, which confirms that hydroxyl radicals are more powerful oxidants than sulfate radicals. The complete removal of organic pollution from natural waters can be accomplished by direct chemical oxidation via hydroxyl radicals generated from photocatalytic decomposition of H$_2$O$_2$.

Keywords: Tannic acid; UV/persulfate; photo-fenton; sulfate radicals; hydroxyl radicals; degradation; mineralization

1. Introduction

Tannic acid (penta-m-digallolyl glucose) (TA) is the simplest principal member of a specific group of hydrolysable tannins [1–3]. The formula of commercial TA, C$_{76}$H$_{52}$O$_{46}$ (Figure 1), involves a large number of reactive functional groups, such as hydroxyl and phenolic hydroxyl. It is a water-soluble polyphenolic material with high molecular weights, between 500 and 3000 Da [4,5]. TA is a natural compound found in bananas, sorghum, coffee, and tea [6,7]. It is also found in industrial wastewaters, which is an emerging problem because of their harmful influence on natural ecosystems [5,8]. It causes liver, kidney, and central nervous system problems due to its high toxicity [9–11].
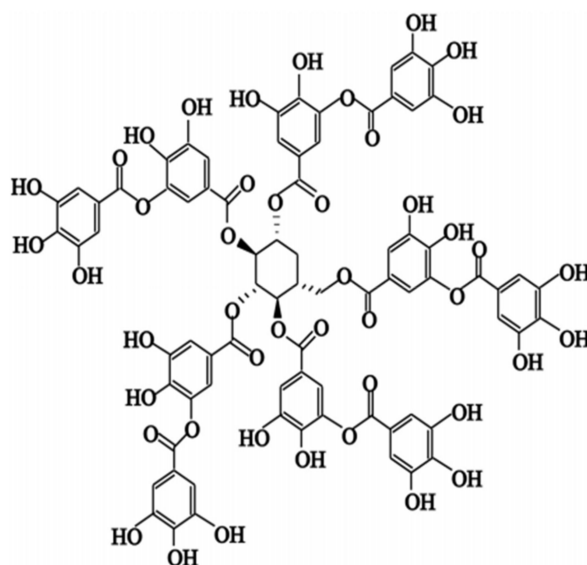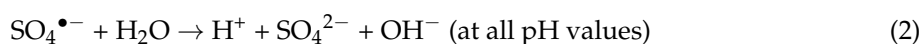
Molecular structure

Formula: $C_{76}H_{52}O_{46}$
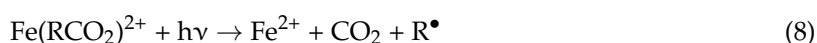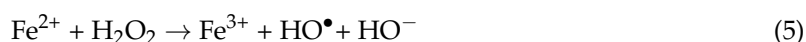
Molecular weight: 1701.2 g/mol

Figure 1. Structure and properties of Tannic Acid.

TA is recalcitrant to conventional biological treatments and other methods [8,12–16]. In our laboratory, electrocoagulation process has been successfully used as a method for treating wastewaters contaminated with TA, but large amounts of precipitates were discharged at the end of the treatment [17]. Recently, advanced oxidation processes (AOPs) based on the generation of hydroxyl radicals (HO$^{\bullet}$) from H_2O_2 have been suggested to eliminate TA [18]. The photochemical system UV/H_2O_2 has also been recently used for TA degradation. This process generates good quality of treated water in comparison with other AOPs, but the amounts of hydroxyl radicals are obtained mainly by H_2O_2 decomposition with UV irradiation, which is a high-energy consumption process. Therefore, it is essential to find more efficient and low-cost alternative technology processes to eliminate TA from water. To achieve this goal, AOPs such as UV/persulfate and photo-Fenton processes have been considered as useful options. AOPs, based on the formation of sulfate radical $SO_4^{\bullet-}$ and hydroxyl radical HO$^{\bullet}$, have been used in in the treatment of wastewater containing bio-recalcitrant organic pollutants/toxicants recalcitrant compounds to convert them into biodegradable products [18–21].

Persulfate ($K_2S_2O_8$) salts decompose in water into persulfate anion ($S_2O_8^{2-}$). It is a very strong oxidant ($E° = 2.05$ V/NHE), which is not selectively reactive and is relatively stable at room temperature [22,23]. However, it is kinetically slow in reacting with many organics at ambient temperatures [24,25]. The photochemical activated degradation of $S_2O_8^{2-}$ ion to sulfate radical ($SO_4^{\bullet-}$) has been used as a technique to accelerate the procedure [24,26,27]. Sulfate radical ($SO_4^{\bullet-}$) is a very strong oxidant for its high standard redox potential (2.5–3.1 V) with a kinetically fast reacting tendency [20,28]. In general, $SO_4^{\bullet-}$ can be generated via photolysis, ultrasonic thermolysis, or activation by transition metals of persulfate or peroxymonosulfate for the oxidation of various organic pollutants [29–34]. UV/$S_2O_8^{2-}$ has been considered as a highly efficient method to destruct different organic pollutants [35,36]. The peroxydisulfate chemistry can be demonstrated by the following equations [24,37,38]:

$$S_2O_8^{2-} + h\nu \rightarrow 2SO_4^{\bullet-} \tag{1}$$

$$SO_4^{\bullet-} + H_2O \rightarrow H^+ + SO_4^{2-} + OH^- \text{ (at all pH values)} \tag{2}$$

$$SO_4^{\bullet-} + OH^- \rightarrow HO^{\bullet} + SO_4^{2-} \text{ (at alkaline pH values)} \tag{3}$$

$$SO_4^{\bullet-} \text{ or } HO^{\bullet} + \text{pollutant} \rightarrow \text{degradation of pollutant} \tag{4}$$

$HO^{\bullet}$ are powerful oxidants (E° = 2.80 V/NHE), which react immediately and non-selectively with organic pollutants in water. It can be generated by a chemical process (Fenton (H_2O_2/Fe^{2+}) [39], photochemical processes UV/TiO_2 [40], UV/H_2O_2 [41,42], photo-Fenton ($UV/H_2O_2/Fe^{2+}$) [43,44], and electrochemical (anodic oxidation, electro-Fenton) [45,46]. This process represents the decomposition of hydrogen peroxide into $HO^{\bullet}$, which occurs through two routes: (1) Catalytic decomposition by Fe^{2+} (Equations (5)) and (2) photodecomposition by UV irradiation at 254 nm (Equation (6)). Additionally, there is the production of further $HO^{\bullet}$ by photo-reduction of ferric to ferrous iron (Equation (7)), combined with H_2O_2 photolysis (Equation (6)), or by photolysis of complexes formed between the organic compounds or their intermediates with Fe^{3+} (Equation (8)) [41,47,48].

$$Fe^{2+} + H_2O_2 \rightarrow Fe^{3+} + HO^{\bullet} + HO^{-} \tag{5}$$

$$H_2O_2 + h\nu \rightarrow 2HO^{\bullet} \tag{6}$$

$$Fe(OH)^{2+} + h\nu \rightarrow Fe^{2+} + HO^{\bullet} \tag{7}$$

$$Fe(RCO_2)^{2+} + h\nu \rightarrow Fe^{2+} + CO_2 + R^{\bullet} \tag{8}$$

As a result, the photo-Fenton process is reported to be effective in removing several varieties of pollutants such as pesticides, dyes, and pharmaceuticals [49–52]. The effectiveness of these techniques is greatly improved by the addition of a catalyst or an oxidant.

The aim of this study is to realize the degradation of TA aqueous solution by UV/persulfate and photo-Fenton processes. Besides, the effect of different factors such as initial pH, oxidant dosage, ferrous iron dose, initial TA content, and temperature on the performance of degradation and mineralization by UV/persulfate and photo-Fenton processes was also evaluated.

2. Materials and Methods

2.1. Chemicals

Tannic acid ($C_{76}H_{52}O_{46}$) was of analytical grade supplied from Sigma-Aldrich Hydrogen peroxide was a 30% solution (*w/w*) (AR grade, Fluka). All the other chemicals including $FeSO_4 \cdot 7H_2O$, $K_2S_2O_8$, H_2SO_4, NaOH, EtOH, t-BuOH, and Na_2SO_3 were of analytical grade and were ordered from Sigma-Aldrich or Fluka.

2.2. Analytical Methods

The total organic carbon (TOC) content of the samples was measured with a TOC-5050 analyzer (Shimadzu Corporation, Kyoto, Japan). Samples taken from treated solutions were filtered with 0.20 µm polytetrafluoroethylene (PTFE) filters before analysis. The UV absorbance of TA aqueous samples was measured using a UV-Visible spectrophotometer by a 1 cm quartz cells at 276 nm. The solution pH was determined with a Micronal pH meter (model B474). TA was analyzed by HPLC using a Nucleosil C18 column (mobile phase, 60% water 40% acetonitrile; flow rate, 0.50 mL min^{-1}) with UV detector at 276 nm.

2.3. UV/$S_2O_8^{2-}$ and UV/H_2O_2/Fe^{2+} Processes

The photochemical experiments were carried out in the photo-reactor (pyrex) of 2 L capacity equipped with a 125-W Heraeus Noblelight (TNN 15/32) mercury vapor lamp, a magnetic stirrer, and a thermometer. The lamp was located in a quartz sleeve at the center of the reactor in an axial position and emitting at 254 nm. 1 L of TA aqueous solution was added into the reactor in each experiment. The solution pH was adjusted to the desired values by addition of sodium hydroxide or sulfuric acid. Then, $K_2S_2O_8$ (UV/persulfate) or $FeSO_4 \cdot 7H_2O$ (photo-Fenton) were directly added to the photoreactor at the beginning of each experiment. After switching on the lamp, a precise amount of hydrogen peroxide (30%) was immediately added to 1 L of TA aqueous solution (for photo-Fenton process). All

the experiments were performed in duplicate. Samples of 10 mL were withdrawn at predetermined time intervals and immediately quenched with Na_2SO_3. The samples were filtered through 0.20 μm polytetrafluoroethylene (PTFE) filters and then tested to determine the pH, TOC, and absorbance at wavelengths of 276 nm in duplicate.

3. Results and Discussion

The efficiency of UV/persulfate (UV/PS) and photo-Fenton (UV/PF) methods was evaluated by following monitoring UV absorbance at 276 nm (a typical UV-visible spectrum of TA aqueous solution presents two bands at 210 nm and 276 nm) and TOC. The absorbance at 276 nm is used to follow the degradation of TA and its aromatic intermediates (% aromatics removal $= \frac{A^0_{\lambda=276\ nm} - A^t_{\lambda=276\ nm}}{A^0_{\lambda=276\ nm}} \times 100$, where $A^0_{\lambda=276\ nm}$ and $A^t_{\lambda=276\ nm}$ are absorbencies measured at 276 nm at t = 0 s and instant t). TOC is used to evaluate the mineralization of the organic content (% TOC removal $= \frac{TOC^0 - TOC^t}{TOC^0} \times 100$, where TOC^0 and TOC^t are TOC measured at t = 0 s and instant t). Persulfate, hydrogen peroxide, ferrous iron and TA concentrations, temperature, and initial pH are the main factors to achieve the highest TA degradation and mineralization yields.

3.1. Comparitive Study of TA Degradation under Various Processes

An initial comparative study on the degradation of TA aqueous solution by six different processes including chemical oxidation by $S_2O_8^{2-}$ alone, chemical oxidation by H_2O_2 alone, direct UV irradiation, UV/H_2O_2, $UV/S_2O_8^{2-}$, and $UV/H_2O_2/Fe^{2+}$ was performed at the same operating conditions (temperature, pH and initial concentrations). The experimental results were compared in Figure 2. According to Figure 2, only 4.22%, 5.35%, and 9.86% of aromatics were reduced by $S_2O_8^{2-}$ alone, H_2O_2 alone and direct UV irradiation, respectively during 120 min. These results indicate that the TA degradation by $S_2O_8^{2-}$ alone, H_2O_2 alone and direct photolysis irradiation was very inefficient, which reveals the direct reactions of persulfate or H_2O_2 with TA in water are generally slow oxidative kinetics. However, combining UV irradiation with H_2O_2 oxidation (UV/H_2O_2) achieved more than 29% of aromatics removal after 120 min.
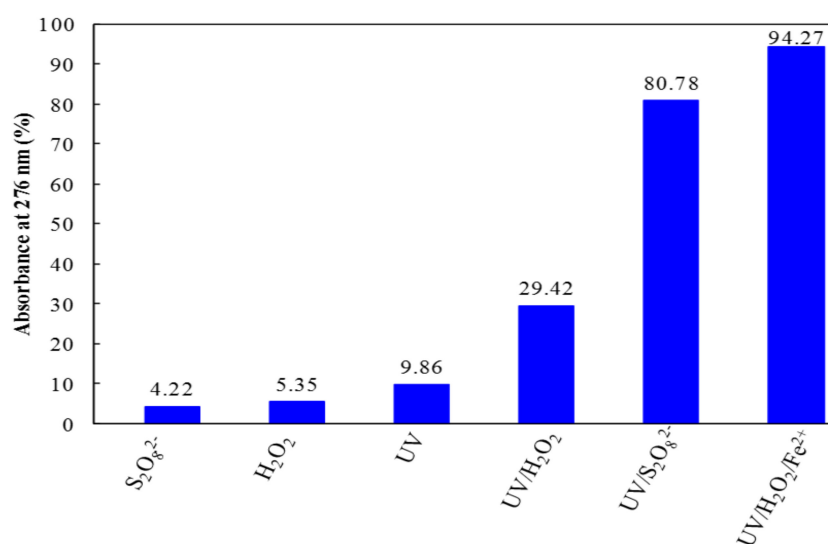

Figure 2. Comparison of TA degradation for 120 min reaction time by different processes including $S_2O_8^{2-}$ alone ($[S_2O_8^{2-}]$ = 53.1 mM), H_2O_2 alone ($[H_2O_2]$ = 29.4 mM), UV irradiation alone (λ = 254 nm), UV/H_2O_2 (λ = 254 nm, $[H_2O_2]$ = 29.4 mM), $UV/S_2O_8^2$ (λ = 254 nm, $[S_2O_8^{2-}]$ = 53.1 mM), and $UV/H_2O_2/Fe^{2+}$ (λ = 254 nm, $[Fe^{2+}]$ = 0.18 mM and $[H_2O_2]$ = 29.4 mM). Experimental conditions: [TA] = 0.1 mM, initial pH (pH = 3.4), T = 25 °C.

This indicates that the combination of hydrogen peroxide with UV radiation enhanced TA degradation. This is because of the $HO^{\bullet}$ radicals produced from UV photolysis of H_2O_2. The above results implied that UV/H_2O_2 process is more efficient than direct UV irradiation and H_2O_2 oxidation alone, but it was not very effective to reach complete removal of TA and its degradation intermediates.

As can be observed from Figure 2, high TA degradation yields can be reached by UV/PS and photo-Fenton oxidation processes, respectively. For a reaction time of 120 min, the highest aromatics removal efficiency was measured as 80.78% for UV/PS and 94.27% for photo-Fenton. This result indicates that TA degradation could be improved by incorporating persulfate ($K_2S_2O_8$) or H_2O_2 and ferrous iron (H_2O_2/Fe^{2+}) to TA aqueous solutions under UV radiation. This enhancement is due to the generated radical species from UV photolysis of persulfate (Equations (1)) or from UV photolysis of the H_2O_2 and from the Fenton reaction (Equations (5) and (6)). In this study, UV/PS and photo-Fenton processes have a higher efficiency to degrade TA than the other four processes ($S_2O_8{}^{2-}$ alone, H_2O_2 alone, UV irradiation, and UV/H_2O_2).

3.2. Influence of Radical Species

To realize the contribution of the oxidizing species ($SO_4{}^{\bullet-}$ and $HO^{\bullet}$) in the efficiency of UV/PS and photo-Fenton processes, two alcoholic radical scavengers, ethanol (EtOH) and tert-butyl alcohol (t-BuOH), were added to TA aqueous solutions. So, alcohol with alpha H (EtOH) can quench both hydroxyl and sulfate radicals; whereas, alcohol with no alpha H (t-BuOH) can mainly scavenge hydroxyl radicals and poorly react with sulfate radicals. In this study, alcohol (EtOH, t-BuOH) concentration used was 50 mM. Figure 3 illustrates the influence of EtOH and t-BuOH as radical scavengers on TA degradation efficiency during UV/PS and $UV/H_2O_2/Fe^{2+}$ processes. As Figure 3 shows, TA degradation was significantly decreased by the addition of alcohols in both processes. The degradation of TA in UV/PS process was 96% without any radical scavenger (see Figure 3a). However, the addition of EtOH and t-BuOH has reduced the efficiencies to 11% and 60%, respectively, within 60 min, compared to the degradation observed in the absence of both scavengers. The results confirmed that the addition of EtOH has diminished the degradation efficiency much more than the same amount t-BuOH.

These observations imply that in the case of t-BuOH addition, hydroxyl radical $HO^{\bullet}$ was scavenged and TA was degraded by sulfate radical $SO_4{}^{\bullet-}$, while in the case of EtOH addition, both $SO_4{}^{\bullet-}$ and $HO^{\bullet}$ were scavenged, which lead to a low TA degradation yield. In order to evaluate the contribution of $HO^{\bullet}$ radicals into TA degradation, t-BuOH was introduced into the photo-reactor during photo-Fenton degradation of TA. As can be seen in Figure 3b, the addition of 50 mM t-BuOH decreased TA degradation yield from 98% (without scavengers) to 16% after 60 min reaction. This confirms that TA degradation occurs mainly via chemical oxidation with hydroxyl radicals during photo-Fenton process.

These results confirmed that the higher aromatics removals obtained in the previous experiments, when US/PS and photo-Fenton processes were used, is mainly due to the oxidation of TA and its aromatics intermediates by radical oxidizing species ($SO_4{}^{\bullet-}$ and $HO^{\bullet}$). Furthermore, it is clear that when UV/PS process is used, not only sulfate radicals, $SO_4{}^{\bullet-}$ contribute in the degradation of TA, but also hydroxyl radicals, $HO^{\bullet}$ are involved in TA degradation since the addition of EtOH and t-BuOH decreased TA degradation yield. Considering that t-BuOH is generally used as $HO^{\bullet}$ scavenger and EtOH can scavenge both $SO_4{}^{\bullet-}$ and $HO^{\bullet}$ radical species, it can be concluded that 60% of TA molecules are degraded by $HO^{\bullet}$ radicals, and only 30–40% of TA molecules are degraded by $SO_4{}^{\bullet-}$ radicals.
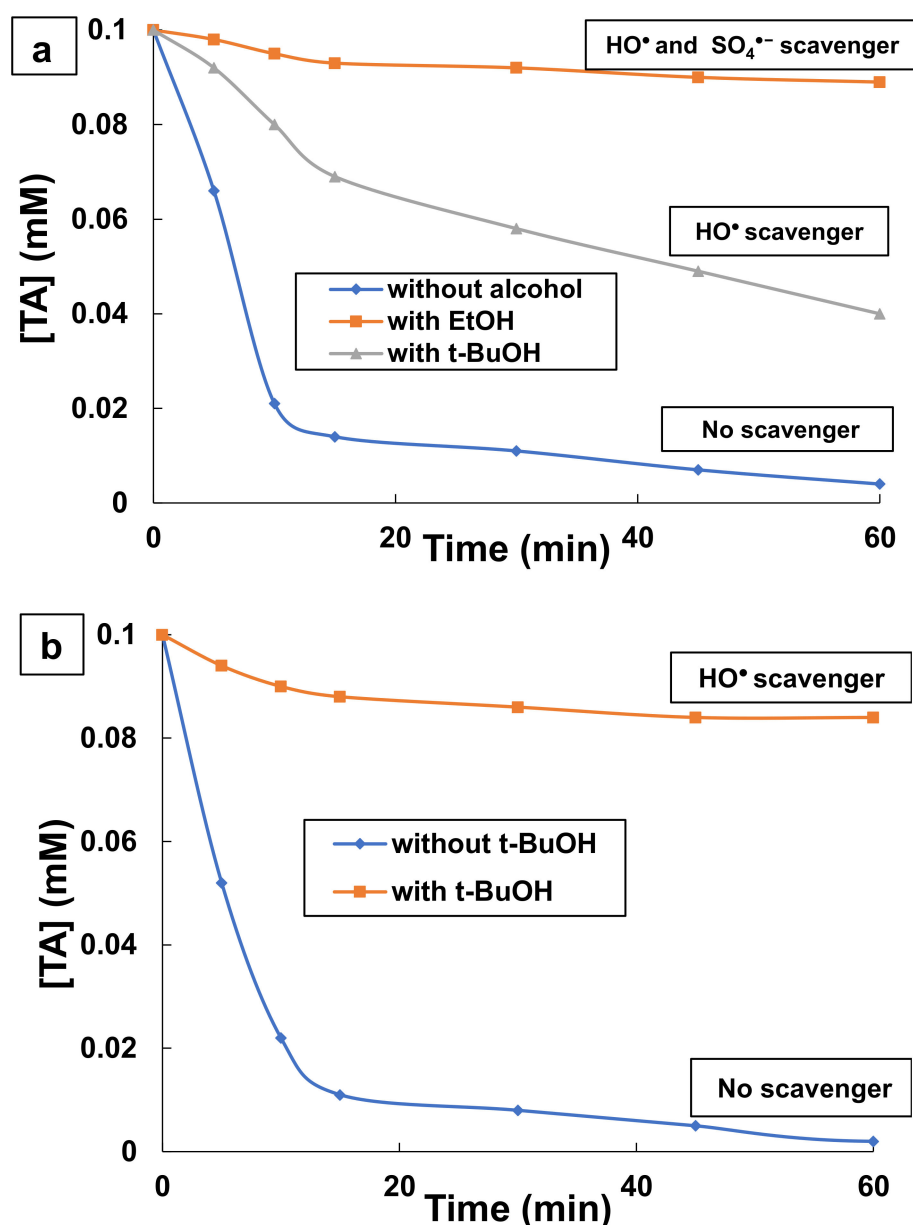
Figure 3. Effect of EtOH and t-BuOH as radical scavengers on TA degradation efficiency during (**a**) UV/persulfate and (**b**) photo-Fenton oxidation. Experimetal conditions: ((**a**) UV/PS: [TA] = 0.1 mM, [EtOH] = 50 mM, [t-BuOH] = 50 mM, [K$_2$S$_2$O$_8$] = 53.1 mM, pH = 9 and T = 25 °C; (**b**) UV/H$_2$O$_2$/Fe^{2+}: [TA] = 0.1 mM, [t-BuOH] = 10 mM, [H$_2$O$_2$] = 29.4 mM, [Fe^{2+}] = 0.18 mM, pH = 3, and T = 25 °C).

3.3. Influence of Ph

It is noteworthy to mention that pH effectively controls the behavior of AOPs [42,53,54]. The UV/persulfate and photo-Fenton processes are heavily dependent on the pH of a solution [44,55–57]. In this study, the effect of initial pH on the photo-degradation of TA through both UV/persulfate (UV/PS) and photo-Fenton (UV/H$_2$O$_2$/Fe^{2+}) processes was examined at pH 3, 5, 7, 9, and 10. Figure 4 represents the changes of aromatics and TOC removals during the treatment of aqueous solutions containing 0.1 mM TA by UV/PS and photo-Fenton processes at different initial pH values.
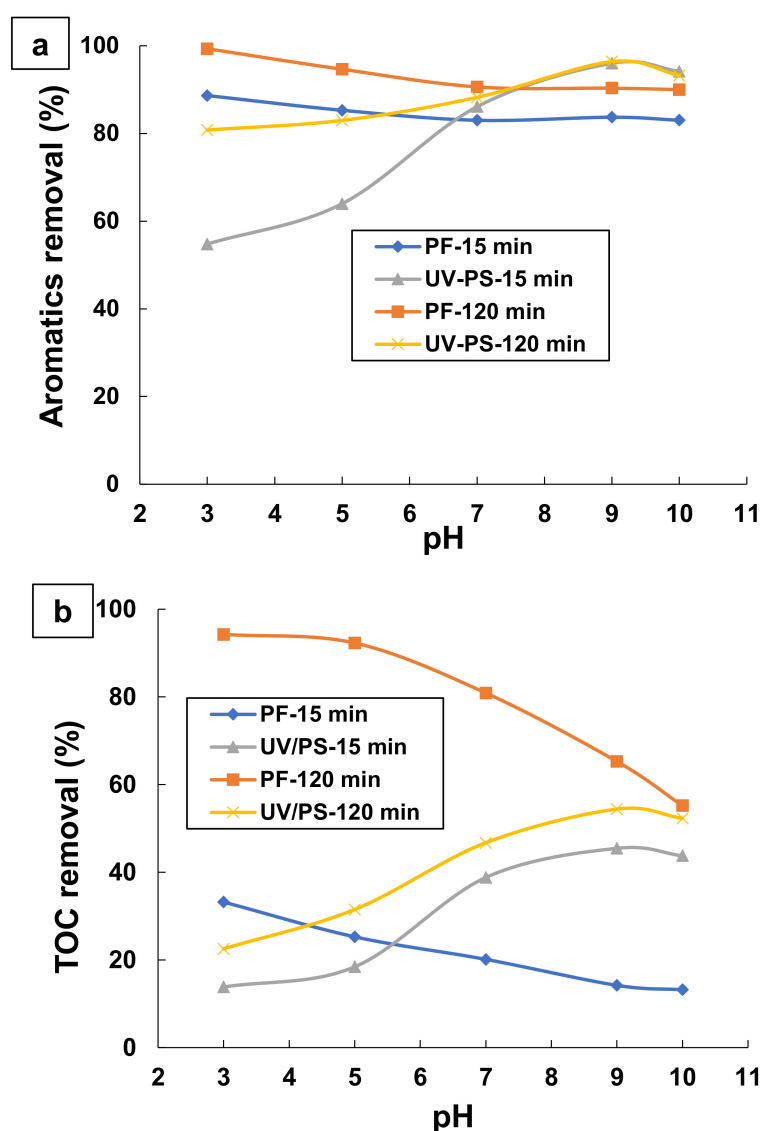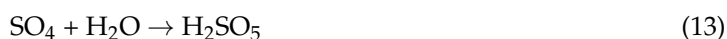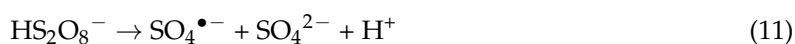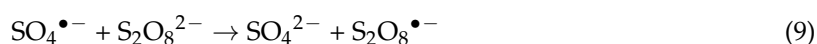
Figure 4. Influence of initial pH on the changes of: (**a**) aromatics removal, and (**b**) TOC removal, during the treatment of 0.1 mM TA by UV/PS and UV/H_2O_2/Fe^{2+} processes. Experimental conditions: (UV/PS: [$K_2S_2O_8$] = 53.1 mM, pH = 3–10 and T = 25 °C; UV/H_2O_2/Fe^{2+}: [H_2O_2] = 29.4 mM, [Fe^{2+}] = 0.18 mM, pH = 3–10, and T = 25 °C).

In the UV/PS process, aromatics and TOC removals were influenced by the initial pH as demonstrated in (Figure 4a,b). The highest efficiency is obtained at an initial pH of 9 and 10. The results suggested that the alkaline conditions were more favorable than neutral and acidic conditions during the degradation of TA. A similar finding was reported in other studies relevant to these observations [57–59]. An increase of pH from three to nine, the photo-degradation efficiency of TA at 120 min irradiation increased from 80.78 to 96.38% and from 22.55 to 54.41%, respectively, for aromatics removal and TOC removal. In contrast, the rise of pH higher than pH 9 does not have any significant influence on the kinetics and TOC removals. This indicates that the highest degradation and mineralization efficiencies of TA by the UV/PS process can be reached at pH nine. These results confirm that very strict conditions (strongly acidic or basic) are less favorable to complete mineralization of TA [57–59].

Thus, the photo-degradation of TA requires a big amount of persulfate radicals and it cannot be carried out at any pH value (see Figure 4b). This may be relative to the abundance of radicals and their nature in the aqueous medium. The literature indicates that increasing the pH increases the

concentration of hydroxyl anions in basic medium [56,60]. The pH effect on the TA photo-degradation by UV/persulfate can be explained by, firstly, base-activated persulfate favored the production of $SO_4^{\bullet-}$ under alkaline condition. $SO_4^{\bullet-}$ doubled, as demonstrated in Equation (1). Second, a high pH, sulfate radicals $SO_4^{\bullet-}$ react with OH^- or H_2O to generate hydroxyl radicals $HO^{\bullet}$ (E° = 2.7 V) based on Equations (2) and (3) [29,61–63]. Thus, $HO^{\bullet}$ is a more powerful oxidant than $SO_4^{\bullet-}$. It should be observed that $HO^{\bullet}$ and sulfates radicals $SO_4^{\bullet-}$ oxidize organic compounds mainly in three ways: (i) Hydrogen abstraction, (ii) addition and substitution of alkanes and aromatics, and (iii) electron transfer from carboxylate groups [64]. On the other hand, in acidic pH, $SO_4^{\bullet-}$ is the predominant radical species in the UV/PS process [60,65]. In our work, the lowest TOC removal efficiency (22%) was observed at pH = 3 after 120 min of treatment (Figure 4b). This can be due to the more selective and less reactive nature of $SO_4^{\bullet-}$ radicals compared to hydroxyl radicals $HO^{\bullet}$. Moreover, at pH < 7, $SO_4^{\bullet-}$ radicals are consumed by $S_2O_8^{2-}$ to form SO_4^{2-} and $S_2O_8^{\bullet-}$, as shown in (Equation (9)). Thus, $SO_4^{\bullet-}$ anions easily degrade TA but cannot complete its mineralization under the acidic conditions. Also, along with radical $SO_4^{\bullet-}$, there are several other sulfur intermediates such as $HS_2O_8^-$, HSO_4^-, SO_4, and H_2SO_5, which are generated and more dominant in the reaction medium according to the following equations (Equations (10)–(13)) [56]:

$$SO_4^{\bullet-} + S_2O_8^{2-} \rightarrow SO_4^{2-} + S_2O_8^{\bullet-} \tag{9}$$

$$S_2O_8^{2-} + H^+ \rightarrow HS_2O_8^- \tag{10}$$

$$HS_2O_8^- \rightarrow SO_4^{\bullet-} + SO_4^{2-} + H^+ \tag{11}$$

$$S_2O_8^{2-} + H^+ \rightarrow HSO_4^- + SO_4 \tag{12}$$

$$SO_4 + H_2O \rightarrow H_2SO_5 \tag{13}$$

In alkaline medium, hydroxyl radicals $HO^{\bullet}$ are formed (Equation (3)). Being very powerful and non-selective, hydroxyl radicals are capable to mineralize TA and its aromatic intermediates. Hence, the maximum aromatics and TOC removals occurred at pH = 9.

For photo-Fenton (UV/H_2O_2/Fe^{2+}) process, removal efficiency reaches a maximum at initial pH of 3. This is similar to a previous investigation [42,48]. Several studies reported that optimal pH for the production of hydroxyl radicals by the photo-Fenton must be in the range three–five [66,67]. It was also demonstrated that at low acid medium (pH > 5), the Fe^{2+} catalyst regeneration becomes very difficult because of $Fe(OH)_3$ precipitation. However, in high acid conditions (pH < 3) protons can function as scavengers for hydroxyl radicals [42]. Additionally, there may be inhibition for the radical forming activity of iron. In this study, the pH is varied from three to 10. UV/H_2O_2/Fe^{2+} process performance was significantly influenced by varying the pH as shown in Figure 4. From Figure 4a, it is obvious that the change in pH had no significant effect on aromatics removal since aromatics removals of 99.3 and 90% at pH values three and 10 after 2 h photo-Fenton treatment of TA. However, TOC removal during UV/H_2O_2/Fe^{2+} process decreased as pH increased (see Figure 4b). As shown in Figure 4b, TOC removal remains almost constant with the increasing of initial pH from pH = 3 to pH = 5. In contrast, when the pH of the reaction was higher than five (neutral or alkaline pH), the TOC removal efficiency rapidly decreased as pH increased. After 2 h of treatment, the obtained percentage of TOC removal was 94.27, 92.29, 80.9, 65.28, and 55.2% at pH 3, 5, 7, 9, and 10, respectively. The findings demonstrated that aromatics were completely degraded into aliphatic intermediates by the photo-Fenton process for acid and neutral mediums, but the degradation was incomplete in the alkaline medium. These results can be interpreted the easier and rapid decomposition of H_2O_2 hydroxyl radical in acidic medium. In addition, the competitive reactions to H_2O_2 photo-reduction such as the consumption of hydroxyl radicals by the protons, the dismutation of hydrogen peroxide and the duplication of hydroxyl radicals are negligible under these conditions. This indicated that the majority of H_2O_2 is decomposed into an important amount of hydroxyl radicals. Consequently, this condition is the most favorable for complete treatment of TA by the photo-Fenton process. However, if

the solution pH is too high (basic medium), H_2O_2 reacts with hydroxide anions to generate water and hydroperoxide anion (HO_2^-) (Equation (14)). At neutral and alkaline pH, precipitation of ferric ions limits the regeneration of Fe^{2+} catalyst. These results are in good agreement with those mentioned in previous reports [42,53]. In this work, pH = 3 was selected as the optimal pH in order to provide a favorable condition for higher mineralization efficiency.

$$H_2O_2 + HO^- \rightarrow H_2O + HO_2^- \tag{14}$$

From the above results, the pH values of three and nine were found to be the optimum pH values for photo-Fenton and UV/PS and processes, respectively.

3.4. Influence of Persulfate Dose

The initial persulfate concentration is an important parameter in the destruction of organic pollutants by UV/PS [24,68]. For this approach, some experiments were done with various PS doses in the range of 17.70–70.80 mM using 0.1 mM TA at pH 9 and a temperature of 25 °C. The results are shown in Figure 5. As it can be seen in Figure 5a, high aromatics removals (>94%) were achieved independently of PS concentration. This indicates that persulfate concentrations higher than 17.70 mM are capable to degrade almost completely TA and its aromatic intermediates.

However, TOC removal depends on PS concentration as demonstrated in Figure 5b. The increase of PS content from 17.70 to 53.10 mM led to increase the TOC removal from 32.97 to 54.41% after a 1 h treatment. PS is a source of sulfate and hydroxyl radicals in the UV/PS process, and more reactive radicals would be generated to degrade TA at higher PS doses. This indicates that an increase of PS dose up to 53.1 mM was able to mineralize more organics. A dose of PS higher than 53.10 mM led to the decrease in TOC removal. It seems that PS dose of 53.10 mM is considered optimal for the treatment of 0.1 mM TA aqueous solution by the UV/PS process. Increasing the persulfate dose above 53.10 mM (optimal dose) resulted in a decrease in TA degradation efficiency. This can be explained by the fact that excessive amount of persulfate ($S_2O_8^{2-}$) in the solution can react with sulfate radicals ($SO_4^{\bullet-}$) to form less reactive species such as persulfate radicals [56,61,69–71]. This, in turn, reduces the efficiency of the process, as explained in Equations (9) and (15).

$$SO_4^{\bullet-} + SO_4^{\bullet-} \rightarrow S_2O_8^{2-} \tag{15}$$

These experimental results are similar to the results obtained by Hori et al. [72] for the degradation of perfluorooctanoic acid (PFOA) using UV/PS process (50 mM persulfate were used).
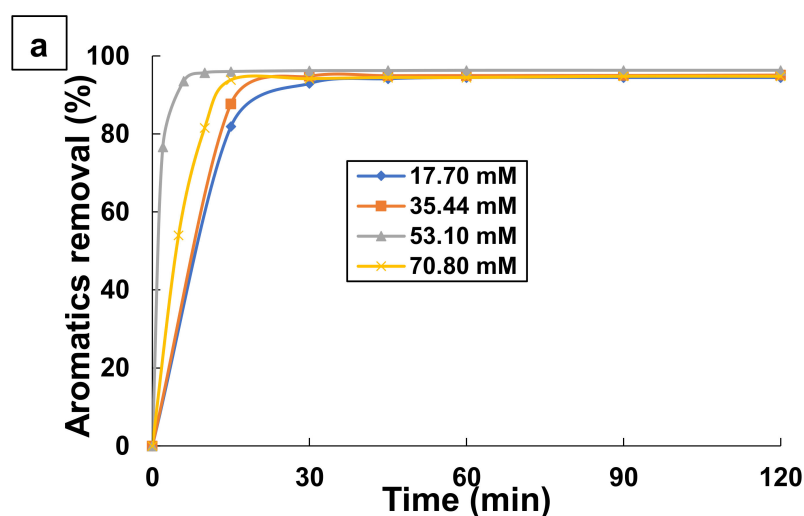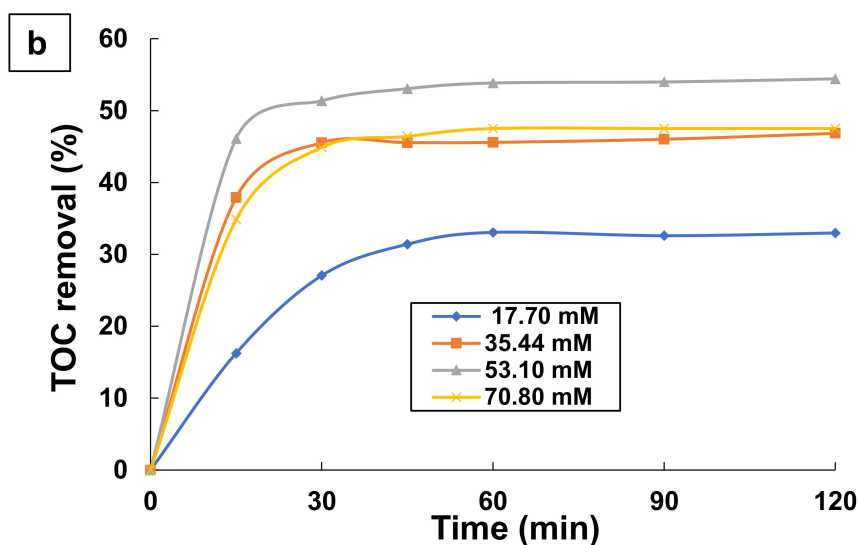
Figure 5. *Cont.*

Figure 5. Effect of persulfate dose on the changes with time of: (**a**) Aromatics removal, and (**b**) TOC removal by UV/PS process. Experimental conditions: [TA] = 0.1 mM; [PS] = 17.70–70.80 mM; T = 25 °C; and pH = 9.

3.5. Influence of Hydrogen Peroxide and Ferrous Iron Concentrations

The amount of hydrogen peroxide and ferrous ions are the main factors affecting the cost of the operation and the process efficiency for many wastewater treatment facilities by Fenton and phot-Fenton processes [73,74]. Photo-Fenton process efficiency can be assessed readily in terms of both the absolute concentration of reagents (hydrogen peroxide and ferrous ions) and the weight ratio ($[H_2O_2]/[Fe^{2+}]$). Several researches affirm that the performance of photo-Fenton process to degrade organic matter present in water is mainly related to the production of hydroxyl radicals by chemical and photochemical decomposition of hydrogen peroxide [41,43]. For this subject, some experiments were conducted at different initial oxidant concentrations using 0.1 mM TA at optimum pH 3 and at a room temperature of 25 °C. Ferrous iron concentration and hydrogen peroxide concentration were examined in the range of 0–0.27 mM and 14.7–58.8 mM, respectively, for TA degradation. Figures 6 and 7 show the effect of ferrous iron and hydrogen peroxide concentrations on aromatics and TOC removals during the treatment of TA by photo-Fenton process.

As it can be observed in Figures 6a and 7a, aromatics removal during the treatment of TA does not depend on the initial contents of ferrous ions and hydrogen peroxide. There is no effect on both the kinetic and the efficiency of absorbance percentage removal. Indeed, over 94% of absorbance reduction was reached in any concentration of ferrous ions and hydrogen peroxide. Thus, it can be concluded that a total disappearance of TA was obtained with the addition of ferrous ions and hydrogen peroxide within the first 60 min of treatment by photo-Fenton process. However, without the addition of a catalyst, 69.42% of absorbance removal could be achieved in UV/H_2O_2 process after 6 h of treatment (Figure 6a). It should be noted that a partial mineralization was obtained under these experimental conditions. These results indicate that ferrous ions are excellent catalysts and a small catalytic amount may be sufficient to decompose H_2O_2 efficiently into hydroxyl radicals $HO^\bullet$. That is why the H_2O_2 concentration is higher than Fe^{2+} in all the experiments. In contrast, Figures 6b and 7b show that the ferrous iron and hydrogen peroxide concentrations have an important effect on the rate of TOC removal during the photo-Fenton treatment. In fact, the incorporation of Fe^{2+} enhanced the efficiency of UV/H_2O_2 for TA degradation (see Figure 6b). It is noticed that, in the presence of Fe^{2+} catalyst, the degradation efficiency is more than 80% after 120 min treatment, while in the absence of Fe^{2+} catalyst, the efficiency of the organic compounds degradation is less than 58% for 420 min of reaction time. Thus, the absence of ferrous iron during the mineralization of TA resulted in the latter's slow degradation. This could be due to the retarding production of excessive generated reactive radicals.

However, by adding ferrous iron, the TOC removal increases from 80.15 to 94.27% after increasing the Fe^{2+} dose from 0.09 mM to 0.18 mM, and then it remains constant above this latter concentration.
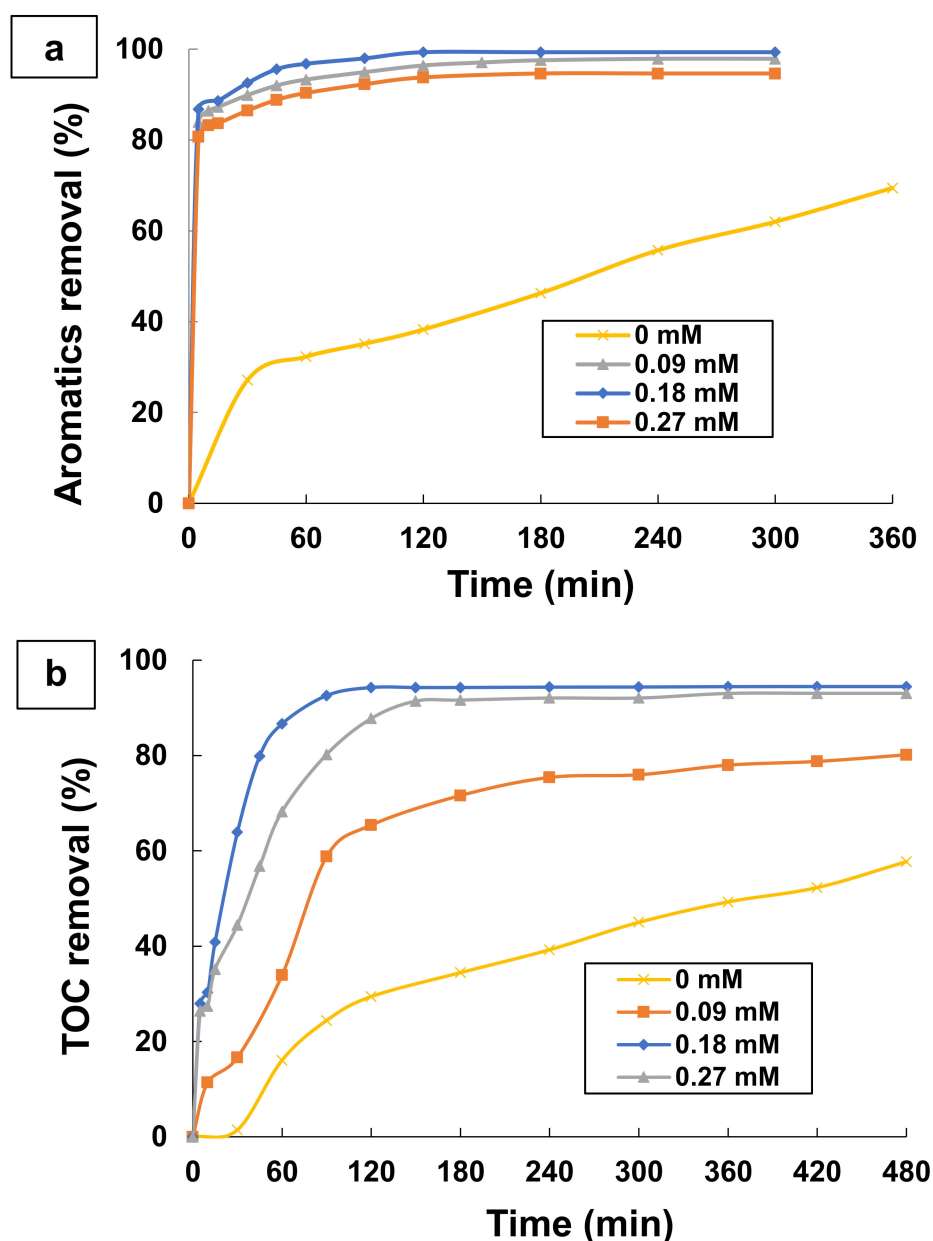

Figure 6. Effect of Fe^{2+} amount on (**a**) Aromatics removal and (**b**) TOC removal by photo-Fenton process $(UV/H_2O_2/Fe^{2+})$. Experimental conditions: [TA] = 0.1 mM; $[Fe^{2+}]$ = 0–0.27 mM; $[H_2O_2]$ = 29.4 mM; T = 25 °C; and pH = 3.

Moreover, the kinetic of TOC removal decreases to a dose of 0.27 mM. Hence, an almost complete conversion of TA was achieved after 120 min of the treatment of TA by photo-Fenton process for 0.18 mM of ferrous iron. These results can be interpreted by the fact that the addition of low amounts of ferrous iron (0.09 mM) does not enhance the performance of photo-Fenton process in wastewater treatment. In this case, a small content of hydroxyl radicals results mainly from the photodecomposition of hydrogen peroxide by UV light and it causes a slow removal in the mineralization. Besides, a gradual increase in the concentration of ferrous ions to 0.18 mM increases the concentration of hydroxyl radicals $HO^{\bullet}$ in the aqueous medium through the photo Fenton process, under the Fenton reaction, to form ferric ions (Equation (5)) and by the photo-reduction of $Fe(OH)^{2+}$ complex (Equation (7)). Moreover,

when high amounts of Fe^{2+} are added to the wastewater, the regeneration of the catalyst (Fe^{2+} ions) from Fe^{3+} ions becomes slow due to the precipitation of ferric hydroxide $Fe(OH)_3$, which prevents the penetration of UV light into the reaction medium and therefore it reduces the quantum efficiency of the UV lamp. Consequently, this inhibits the generation of hydroxyl radicals by ferrous iron. In addition, the use of a much higher concentration of Fe^{2+} could lead to the self-scavenging of hydroxyl radical $HO^\bullet$ by converting it to hydroxyl ions HO^- during the oxidation of Fe^{2+} (Equation (16)). From these results, we can deduce that a 0.18 mM dose of ferrous ions is optimal for a better treatment of aqueous solutions containing 0.1 mM of TA at pH 3.0 and 29.4 mM of H_2O_2, using the photo-Fenton process.

$$Fe^{2+} + HO^\bullet \rightarrow Fe^{3+} + HO^- \tag{16}$$

Similar behavior is noticed in the case of hydrogen peroxide dosage (Figure 7b). The addition of initial hydrogen peroxide concentration from 14.7 to 29.4 mM resulted in an increase in mineralization extents from 84.22% to 94.27% of TOC removal after 120 min of treatment, as seen in Figure 7b. A low concentration of H_2O_2 did not allow achieving complete mineralization of TA in the photo-Fenton treatment. This can be explained by Equation (6). Increasing the amount of H_2O_2 up to 29.4 mM caused considerable efficiency improvement because of more reactive radical generation (Equations (5) and (6)), which strongly enhanced the efficiency of TA degradation. Further increase of the H_2O_2 dose, greater than 29.4 mM, decreased the mineralization efficiency from 94.27% to 80.19% after 120 min of the treatment of TA. After reaching an optimal value, a further boost of H_2O_2 concentration negatively influences the efficiency of the process due to the $OH^\bullet$ scavenging effect of H_2O_2 and recombination of hydroxyl radicals (Equation (17)). In addition, when hydrogen peroxide concentration is elevated, the competitive reactions of hydroxyl radicals with H_2O_2 excess in order to produce $HO_2^\bullet$ (Equations (18) and (19)) consume a considerable amount of $HO^\bullet$ radicals, which leads to a decline in the process efficiency.
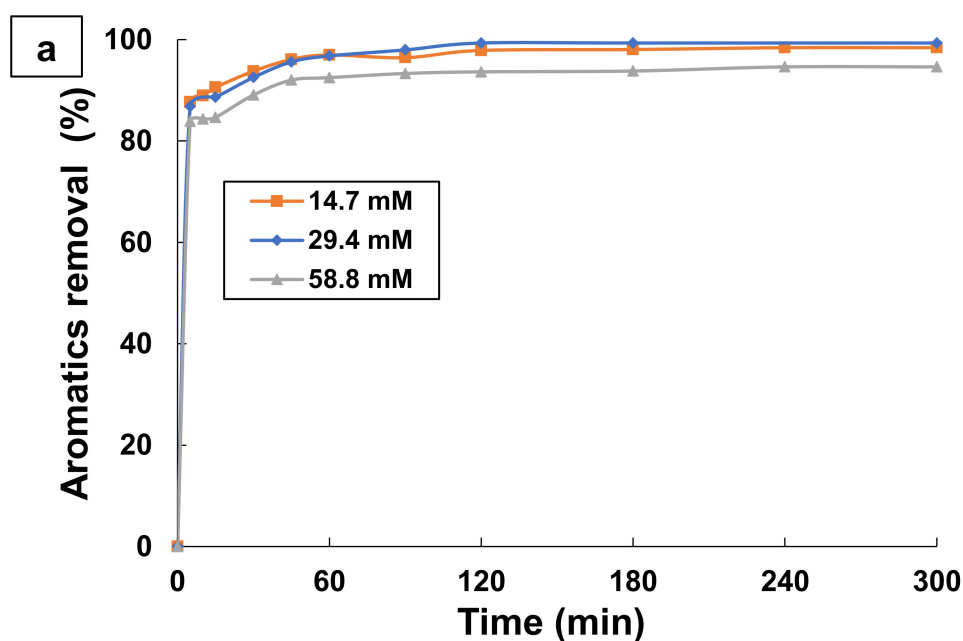
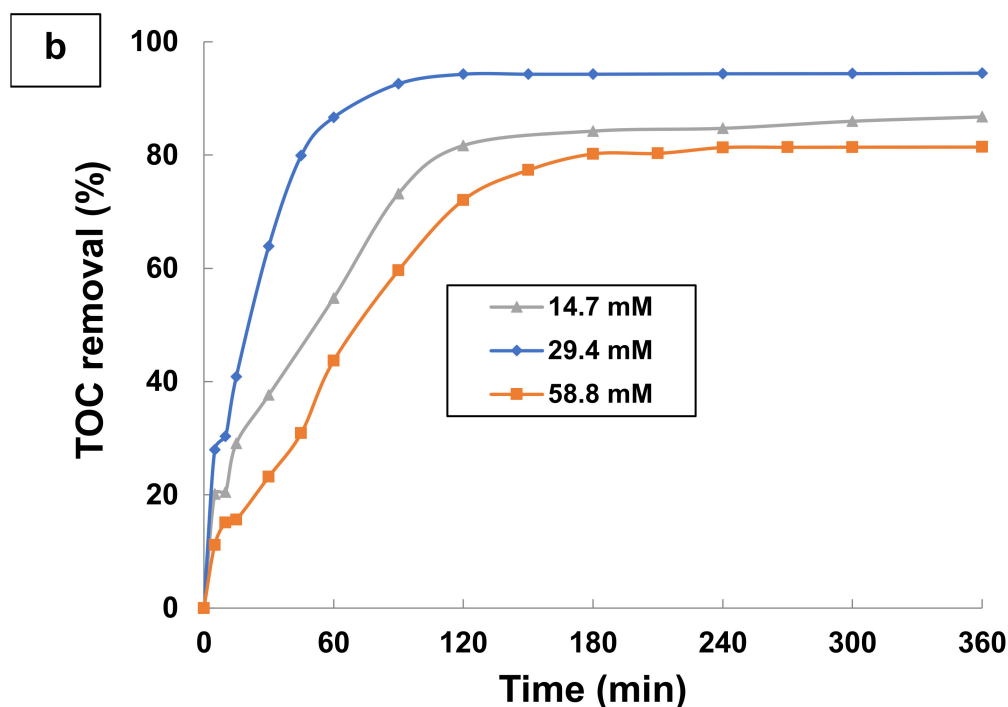$$HO^\bullet + HO^\bullet \rightarrow H_2O_2 \tag{17}$$

$$H_2O_2 + HO^\bullet \rightarrow H_2O + HO_2^\bullet \tag{18}$$

$$HO_2^\bullet + HO^\bullet \rightarrow H_2O + O_2 \tag{19}$$

Figure 7. *Cont.*

Figure 7. Effect of H_2O_2 dose on (**a**) Aromatics removal and (**b**) TOC removal by photo-Fenton process ($UV/H_2O_2/Fe^{2+}$). Experimental conditions: [TA] = 0.1 mM; [H_2O_2] = 14.7–58.8 mM; [H_2O_2]/[Fe^{2+}] = 164; T = 25 °C; and pH = 3.

Therefore, a H_2O_2 dose of 29.4 mM was found to be optimal for a complete disappearance of TA in 60 min and total TOC removal in 120 min in the photo-Fenton oxidation for treating TA wastewater. It was found that both parameters Fe^{2+} and H_2O_2 had a positive effect on the percentage of TOC removal over the studied range. The optimal conditions for the decay absorbance at 276 nm (aromatics removal) and TOC removal of TA were determined as [Fe^{2+}] = 0.18 mM and [H_2O_2] = 29.4 mM. This corresponds to a mass ratio of H_2O_2 dose to Fe^{2+} dose ([H_2O_2]/[Fe^{2+}]) equal to 164.

3.6. Influence of Initial Dose of TA

To study the effect of this parameter, four TA concentrations of 0.05, 0.1, 0.2, and 0.4 mM were tested at optimum conditions determined in previous steps (UV/PS: [$K_2S_2O_8$]/[TA] = 531, pH = 9 and T = 25 °C; $UV/H_2O_2/Fe^{2+}$: [H_2O_2]/[Fe^{2+}] = 164, [H_2O_2]/[TA] = 294, pH = 3, and T = 25 °C). Results presenting final percentage of absorbance and TOC removals for 120 min treatment are illustrated in Figure 8. As shown in Figure 8a, the initial concentration of TA has no significant effect on either the rate or the percentage of aromatics removal during the treatment by UV/persulfate and photo-Fenton processes. In both processes, there is more than 90% of absorbance removal for the different initial concentration of TA in the range 0.05–0.4 mM. However, TOC removal was strongly influenced by the initial concentration of TA, as seen in Figure 8b. An increase in TA concentration from 0.05 to 0.1 mM resulted in an increase in removal efficiency from 42.95 to 54.41% and from 85.44 to 94.27% for the UV/persulfate and photo-Fenton processes, respectively, at 120 min of treatment. Increasing initial concentration of TA from 0.1 to 0.4 mM decreases TOC removal efficiency.

The results obtained can be interpreted as follows: (i) A higher TA dose requires a big amount of oxidants, and thus, the process efficiency decreased with a constant amount of oxidant. The greater of amount in the reaction medium decreases the quantum yield of production of sulfates radicals $SO_4^{\bullet-}$ from $K_2S_2O_8$ and hydroxyl radicals $OH^{\bullet}$ from H_2O_2. This is mainly due to the absorption of a significant amount of UV radiation by the organic molecules, besides, by the coloring of the solution and the formation of a precipitate layer of the jacket of the reactor, which makes difficult the passage of

UV light in organic molecules. It is also due to competition between TA molecules and intermediates compounds generated during the reaction. (ii) A low concentrations of TA and oxidants ($K_2S_2O_8$, Fe^{2+}, and H_2O_2) decrease the probability of collusion between sulfates or hydroxyl radicals and aliphatic intermediates, which makes difficult their mineralization into CO_2 and H_2O. Several authors have found similar observation in their study [44,75–77].
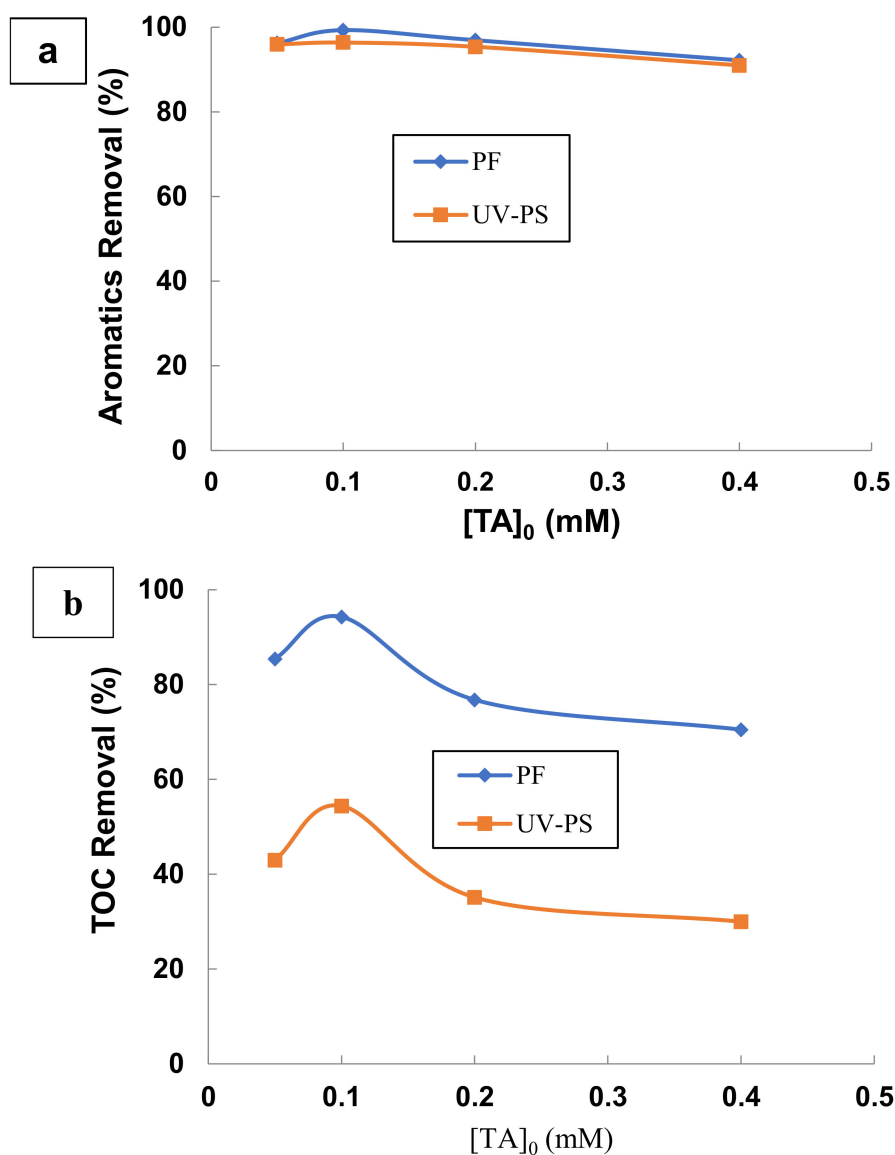

Figure 8. Effect of TA initial concentration on (**a**) aromatics removal and (**b**) TOC removal by UV/persulfate (UV-PS) and photo-Fenton (UV/H_2O_2/Fe^{2+}) processes under optimal conditions. (UV/PS: [TA] = 0.05–0.4 mM, [$K_2S_2O_8$]/[TA] = 531, pH = 9 and T = 25 °C; UV/H_2O_2/Fe^{2+}: [TA] = 86–680 mg L^{-1}, [H_2O_2]/[Fe^{2+}] = 164, [H_2O_2]/[TA] = 294, pH = 3, and T = 25 °C).

From these results, it is concluded that the best performance for the mineralization and degradation of TA by UV/persulfate and photo-Fenton processes is obtained for an initial dose of TA equal to 0.1 mM. This corresponds to a ratio weight equal to 531 and 294 successively for [$K_2S_2O_8$]/[TA] and [H_2O_2]/[TA]. The two ratios are relative to the degradation and the mineralization of TA. It is also clear that aromatics were decomposed into aliphatic intermediates by the photo-Fenton process, but it is more difficult to mineralize TA by the UV/persulfate process. Therefore, the mineralization and degradation of TA by the photo-Fenton process are more effective than by UV/persulfate process.

3.7. Temperature Influence

Table 1 shows the effect of temperature on absorbance decay percentage and TOC removal percentage during the treatment of TA by UV/PS and photo-Fenton processes within 2 h UV irradiation. Temperature was examined in the range of 20–35 °C. The work of this range of temperature does not cause any risk for either UV lamp or the photo-reactor. Results indicated that the increase of temperature from 20 °C to 25 °C increases the percentage of absorbance and TOC removals at 120 min of the treatment. However, the increase of this temperature from 25 °C to 35 °C does not have any significant effect on aromatics and TOC removals during the treatment of aqueous solutions of TA by the UV/PS and photo-Fenton processes.

Table 1. Effect of temperature on UV/PS and photo-Fenton efficiencies during the degradation of TA for 2 h UV irradiation. (UV/PS: $[K_2S_2O_8]/[TA]$ = 531, pH = 9 and T = 20–35 °C; $UV/H_2O_2/Fe^{2+}$: $[H_2O_2]/[Fe^{2+}]$ = 164, $[H_2O_2]/[TA]$ = 294, pH = 3, and T = 20–35 °C).

Temperature (°C)	% ABS Removal		% TOC Removal	
	UV/PS	PF	UV/PS	PF
20 °C	92.4 ± 0.4	94.9 ± 0.6	50.4 ± 0.1	88.9 ± 0.5
25 °C	96.4 ± 0.7	99.3 ± 0.3	54.3 ± 0.2	94.3 ± 0.5
35 °C	95.8 ± 0.3	97.3 ± 0.4	53.6 ± 0.6	93.8 ± 0.5

Thus, the optimum temperature deduced in this study is 25 °C for the treatment of this effluent, so less heating energy should be consumed. This phenomenon can be attributed to increasing the temperature higher than the optimum value (25 °C) accelerates the rate of competitive reactions which consumes sulfates and hydroxyl radicals. Besides, for a low temperature, the sulfates and hydroxyl radicals generated in the reaction medium are not able to degrade TA. Many reports discussed the temperature influence and have found similar results [74,78]. From these results, it can be concluded that UV/persulfate process cannot be a viable option for the treatment of TA in water taking into account its low mineralization yield (54.41%). Further investigations are needed to enhance the performance of UV/PS in the mineralization of organic matter. The photo-Fenton $(UV/H_2O_2/Fe^{2+})$ process achieved more than 99% of aromatics removal and more than 94% of TOC removal. The combination of UV/PS and photo-Fenton can be a good cost-effective method that benefits from the advantages of persulfates (low cost) and the high efficiency of photo-Fenton (high mineralization).

4. Conclusions

The efficiency and operating parameters for the treatment of TA by the UV/persulfate and photo-Fenton were evaluated and compared. The results from this study showed that the performance of photo-Fenton process is significantly superior to that of UV/persulfate process in the degradation of TA aqueous solutions. The optimum conditions obtained for the best degradation were a pH = 9, a persulfate concentration of about 53.10 mM, a TA concentration of 0.1 mM and a temperature of 25 °C for UV/persulfate process and a pH 3, a ferrous iron concentration of 0.18 mM, a hydrogen peroxide concentration of 29.4 mM, a TA concentration of 0.1 mM, and a temperature of 25 °C for the photo-Fenton process. Under optimal conditions, removal efficiency for UV/persulfate and photo-Fenton were 96.38% and 99.32% for absorbance removal and 54.41% and 94.27% for TOC removal, respectively. The results obtained have shown that a more complete mineralization was obtained in the photo-Fenton process. It can be summarized that photo-Fenton process more effective than UV/persulfate process. The efficiency of photo-Fenton can be explained by the catalytic decomposition of H_2O_2 by Fe^{2+} ions, the photo reduction of hydrogen peroxide by irradiation UV and the photo-reduction of hydroxyl iron complex, which lead to the production of higher contents of hydroxyl radicals. Of those hydroxyl radicals, $HO^{\bullet}$ is a more powerful oxidant than sulfates radicals

$SO_4^{\bullet-}$. Even though, PS is widely known to produce less powerful radicals, the fact of having an optimal pH at nine may be easily applied to real cases and the costs of adjusting the pH can be fewer.

References

1. Buzzini, P.; Arapitsas, P.; Goretti, M.; Branda, E.; Turchetti, B.; Pinelli, P.; Ieri, F.; Romani, A. Antimicrobial and antiviral activity of hydrolysable tannins. *Mini-Rev. Med. Chem.* **2008**, *8*, 1179–1187. [CrossRef] [PubMed]

2. Coppo, E.; Marchese, A. Antibacterial activity of polyphenols. *Curr. Pharm. Biotechnol.* **2014**, *15*, 380–390. [CrossRef] [PubMed]

3. Orlowski, P.; Soliwoda, K.; Emilia, T.; Bien, K.; Fruba, A.; Gniadek, M.; Labedz, O.; Nowak, Z.; Celichowski, G.; Grobelny, J.; et al. Toxicity of tannic acid-modified silver nanoparticles in keratinocytes: Potential for immunomodulatory applications. *Toxicol. In Vitro* **2016**, *35*, 43–54. [CrossRef] [PubMed]

4. Erdelyi, K.; Kiss, A.; Bakondi, E.; Bai, P.; Szabo, C.; Gergely, P.; Erdodi, F.; Virag, L. Gallotannin inhibits the expression of chemokines and inflammatory cytokines in A549 cells. *Mol. Pharmacol.* **2005**, *68*, 895–904. [CrossRef] [PubMed]

5. Sun, C.; Xiong, B.; Pan, Y.; Cui, H. Adsorption removal of tannic acid from aqueous solution by polyaniline: Analysis of operating parameters and mechanism. *J. Colloid Interface Sci.* **2017**, *487*, 175–181. [CrossRef] [PubMed]

6. Tomaszewska, E.; Dobrowolski, P.; Winiarska-Mieczan, A.; Kwiecien, M.; Tomczyk, A.; Muszynski, S. The effect of tannic acid on the bone tissue of adult male Wistar rats exposed to cadmium and lead. *Exp. Toxicol. Pathol.* **2017**, *69*, 131–141. [CrossRef] [PubMed]

7. Chakrabarty, T.; Pérez-Manríquez, L.; Neelakanda, P.; Peinemann, K.V. Bioinspired tannic acid-copper complexes as selective coating for nanofiltration membranes. *Sep. Purif. Rev.* **2017**, *184*, 188–194. [CrossRef]

8. Wang, J.H.; Zheng, S.R.; Liu, J.L.; Xu, Z.Y. Tannic acid adsorption on aminofunctionalized magnetic mesoporous silica. *Chem. Eng. J.* **2010**, *165*, 10–16. [CrossRef]

9. Varanka, Z.; Rojik, I.; Varanka, I.; Nemcsók, J.; Ábrahám, M. Biochemical and morphological changes in carp (*Cyprinus carpio* L.) liver following exposure to copper sulfate and tannic acid. *Comp. Biochem. Physiol. C* **2001**, *128*, 467–477. [CrossRef]

10. De Nicola, E.; Meriç, S.; Gallo, M.; Iaccarino, M.; Della, R.C.; Lofrano, G.; Russo, T.; Pagano, G. Vegetable and synthetic tannins induce hormesis/toxicity in sea urchin early development and in algal growth. *Environ. Pollut.* **2007**, *146*, 46–54. [CrossRef]

11. Deng, Y.H.; Wang, L.; Hu, X.B.; Liu, B.Z.; Wei, Z.B.; Yang, S.G.; Sun, C. Highly efficient removal of tannic acid from aqueous solution by chitosan-coated attapulgite. *Chem. Eng. J.* **2012**, *181–182*, 300–306. [CrossRef]

12. Buso, A.; Balbo, L.; Giomo, M.; Farnia, G.; Sandonà, G. Electrochemical removal of tannins from aqueous solutions. *Ind. Eng. Chem. Res.* **2000**, *39*, 494–499. [CrossRef]

13. Cañizares, P.; Pérez, Á.; Camarillo, R.; Llanos, J. Tannic acid removal from aqueous effluents using micellar enhanced ultrafiltration at pilot scale. *Desalination* **2006**, *200*, 310–312. [CrossRef]

14. Rodríguez, H.; de las Rivas, B.; Gómez-Cordovés, C.; Muñoz, R. Degradation of tannic acid by cell–free extracts of Lactobacillus plantarum. *Food Chem.* **2008**, *107*, 664–670. [CrossRef]

15. Pepi, M.; Lampariello, L.R.; Altieri, R.; Esposito, A.; Perra, G.; Renzi, M.; Lobianco, A.; Feola, A.; Gasperini, S.; Focardi, S.E. Tannic acid degradation by bacterial strains *Serratia* spp. and *Pantoea* sp. isolated from olive mill waste mixtures. *Int. Biodeterior. Biodegrad.* **2010**, *64*, 73–80. [CrossRef]

16. Goel, G.; Kumar, A.; Beniwal, V.; Raghav, M.; Puniya, A.K.; Singh, K. Degradation of tannic acid and purification and characterization of tannase from Enterococcus faecalis. *Int. Biodeterior. Biodegrad.* **2011**, *65*, 1061–1065. [CrossRef]

17. Mansouri, K.; Elsaid, K.; Bedoui, A.; Bensalah, N.; Abdel-Wahabb, A. Application of electrochemically dissolved iron in the removal of tannic acid from water. *Chem. Eng. J.* **2011**, *172*, 970–976. [CrossRef]

18. Bensalah, N.; Chair, K.; Bedoui, A. Efficient degradation of tannic acid in water by UV/H$_2$O$_2$ process. *Sustain. Environ. Res.* **2018**, *28*, 1–11. [CrossRef]

19. Adak, A.; Mangalgiri, K.P.; Lee, J.; Blaney, L. UV irradiation and UV-H$_2$O$_2$ advanced oxidation of the roxarsone and nitarsone organoarsenicals. *Water Res.* **2015**, *70*, 74–85. [CrossRef]

20. Avetta, P.; Pensato, A.; Minella, M.; Malandrino, M.; Maurino, V.; Minero, C.; Hanna, K.; Vione, D. Activation of persulfate by irradiated magnetite: Implications for the degradation of phenol under heterogene heterogeneous photo-fentonlike conditions. *Environ. Sci. Technol.* **2015**, *49*, 1043–1050. [CrossRef]

21. Khandarkhaeva, M.; Batoeva, A.; Aseev, D.; Sizykh, M.; Tsydenova, O. Oxidation of atrazine in aqueous media by solar- enhanced Fenton-like process involving persulfate and ferrous ion. *Ecotoxicol. Environ. Saf.* **2017**, *137*, 35–41. [CrossRef] [PubMed]

22. Pérez, S.; Eichhorn, P.; Celiz, M.D.; Aga, D.S. Structural characterization of metabolites of the X-ray contrast agent iopromide in activated sludge using ion trap mass spectrometry. *Anal. Chem.* **2006**, *78*, 1866–1874. [CrossRef] [PubMed]

23. Osgerby, I.T. ISCO technology overview: Do you really understand the chemistry? In *Contaminated Soils, Sediments and Water*; Calabrese, E.J., Kostecki, P.T., Dragun, J., Eds.; Springer: Boston, MA, USA, 2006; Volume 10, pp. 287–308.

24. Saien, J.; Soleymani, A.R.; Sun, J.H. Parametric optimization of individual and hybridized AOPs of Fe^{2+}/H$_2$O$_2$ and UV/S$_2$O$_8^{2-}$ for rapid dye destruction in aqueous media. *Desalination* **2011**, *279*, 298–305. [CrossRef]

25. Velo-Gala, I.; López-Peñalver, J.J.; Sánchez-Polo, M.; Rivera-Utrilla, J. Comparative study of oxidative degradation of sodium diatrizoate in aqueous solution by H$_2$O$_2$/Fe^{2+}, H$_2$O$_2$/Fe^{3+}, Fe (VI) and UV, H$_2$O$_2$/UV, K$_2$S$_2$O$_8$/UV. *Chem. Eng. J.* **2014**, *241*, 504–512. [CrossRef]

26. Guan, Y.H.; Ma, J.; Ren, Y.M.; Liu, Y.L.; Xiao, J.Y.; Lin, L.Q.; Zhang, C. Efficient degradation of atrazine by magnetic porous copper ferrite catalyzed peroxymonosulfate oxidation via the formation of hydroxyl and sulfate radicals. *Water Res.* **2013**, *47*, 5431–5438. [CrossRef] [PubMed]

27. Lutze, H.V.; Bircher, S.; Rapp, I.; Kerlin, N.; Bakkour, R.; Geisler, M.; Schmidt, T.C. Degradation of chlorotriazine pesticides by sulfate radicals and influence of organic matter. *Environ. Sci. Technol.* **2015**, *49*, 1673–1680. [CrossRef] [PubMed]

28. Luo, C.; Ma, J.; Jiang, J.; Liu, Y.; Song, Y.; Yang, Y.; Guan, Y.; Wu, D. Simulation and comparative study on the oxidation kinetics of atrazine by UV/H$_2$O$_2$, UV/HSO$_5^-$ and UV/S$_2$O$_8^{2-}$. *Water Res.* **2015**, *80*, 99–108. [CrossRef]

29. Gao, Y.Q.; Gao, N.Y.; Deng, Y.; Yang, Y.Q.; Ma, Y. Ultraviolet (UV) light-activated persulfate oxidation of sulfamethazine in water. *Chem. Eng. J.* **2012**, *195–196*, 248–253. [CrossRef]

30. Hori, H.; Nagano, Y.; Murayama, M.; Koike, K.; Kutsuna, S. Efficient decomposition of perfluoroether carboxylic acids in water with a combination of persulfate oxidant and ultrasonic irradiation. *J. Fluor. Chem.* **2012**, *141*, 5–10. [CrossRef]

31. Guo, Y.G.; Zhou, J.; Lou, X.Y.; Liu, R.L.; Xiao, D.X.; Fang, C.L.; Wang, Z.H.; Liu, J.S. Enhanced degradation of Tetrabromobisphenol A in water by a UV/base/persulfate system: Kinetics and intermediates. *Chem. Eng. J.* **2014**, *254*, 538–544. [CrossRef]

32. Johnson, R.L.; Tratnyek, P.G.; Johnson, R.O. Persulfate persistence under thermal activation conditions. *Environ. Sci. Technol.* **2008**, *42*, 9350–9356. [CrossRef] [PubMed]

33. Anipsitakis, G.P.; Dionysiou, D.D. Radical generation by the interaction of transition metals with common oxidants. *Environ. Sci. Technol.* **2004**, *38*, 3705–3712. [CrossRef] [PubMed]

34. Antoniou, M.G.; Cruz, A.A.; Dionysiou, D.D. Degradation of microcystin-LR using sulfate radicals generated through photolysis, thermolysis and e-transfer mechanisms. *Appl. Catal. B* **2010**, *96*, 290–298. [CrossRef]

35. Shah, N.S.; He, X.; Khan, H.M.; Khan, J.A.; O'shea, K.E.; Boccelli, D.L.; Dionysiou, D.D. Efficient removal of endosulfan from aqueous solution by UV-C/peroxides: A comparative study. *J. Hazard. Mater.* **2013**, *263*, 584–592. [CrossRef]

36. He, X.; Mezyk, S.P.; Michael, I.; Fatta-Kassinos, D.; Dionysiou, D.D. Degradation Kinetics and mechanism of -lactam antibiotics by the activation of H$_2$O$_2$ and Na$_2$S$_2$O$_8$ under UV-254 nm irradiation. *J. Hazard. Mater.* **2014**, *279*, 375–383. [CrossRef] [PubMed]

37. Soleymani, A.R.; Saien, J.; Bayat, H. Artificial neural networks developed for prediction of dye decolorization efficiency with UV/$K_2S_2O_8$ process. *Chem. Eng. J.* **2011**, *170*, 29–35. [CrossRef]

38. Xiaoyang, C.; Xue, Z.; Yanlai, Y.; Weiping, W.; Fengxiang, Z.; Chunlai, H. Oxidation Degradation of Rhodamine B in Aqueous by UV/S_2O_8 Treatment System. *Int. J. Photoenergy* **2012**, *2012*, 754691. [CrossRef]

39. Bensalah, N.; Khodary, A.; Abdel-Wahab, A. Kinetic and Mechanistic Investigations of Mesotrione Degradation in Aqueous Medium by Fenton Process. *J. Hazard. Mater.* **2011**, *189*, 479–485. [CrossRef]

40. Hua, W.; Bennett, E.R.; Letcher, R.J. Ozone Treatment and the Depletion of Detectable Pharmaceuticals and Atrazine Herbicide in Drinking Water Sourced from the Upper Detroit River, Ontario, Canada. *Water Res.* **2006**, *40*, 259–2266. [CrossRef]

41. Ahmed, B.; Mohamed, H.; Limem, E.; Nasr, B. Degradation and Mineralization of Organic Pollutants Contained in Actual Pulp and Paper Mills Wastewaters by a UV/H_2O_2 Process. *Ind. Eng. Chem. Res.* **2009**, *48*, 3370–3379. [CrossRef]

42. Bedoui, A.; Elsaid, K.; Bensalah, N.; Abdel-Wahab, A. Treatment of Pharmaceutical-Manufacturing Wastewaters by UV Irradiation/Hydrogen Peroxide Process. *J. Adv. Oxid. Technol.* **2011**, *14*, 226–234. [CrossRef]

43. Konstantinou, K.I.; Albanis, A.T. Photocatalytic Transformation of Pesticides in Aqueous Titanium Dioxide Suspensions Using Artificial and Solar Light: Intermediates and Degradation Pathways. *Appl. Catal. B Environ.* **2003**, *42*, 319–335. [CrossRef]

44. Dbira, S.; Bedoui, A.; Bensalah, N. Investigations on the Degradation of Triazine Herbicides in Water by Photo-Fenton Process. *Am. J. Anal. Chem.* **2014**, *5*, 500–517. [CrossRef]

45. Bedoui, A.; Elalaoui, L.; Ahmed, A.W.; Bensalah, N. Photo-Fenton Treatment of Actual Agro-Industrial Wastewaters. *Ind. Eng. Chem. Res.* **2011**, *50*, 6673–6680.

46. Dbira, S.; Bensalah, N.; Cañizares, P.; Rodrigo, M.A.; Bedoui, A. The electrolytic treatment of synthetic urine using DSA electrodes. *J. Electroanal. Chem.* **2015**, *744*, 62–68. [CrossRef]

47. Kavitha, V.; Palanivelu, K. The role of ferrous ion in Fenton and photo-Fenton processes for the degradation of phenol. *Chemosphere* **2004**, *55*, 1235–1243. [CrossRef] [PubMed]

48. Hermosilla, D.; Cortijo, M.; Huang, C.P. Optimizing the treatment of landfill leachate by conventional Fenton and photo-Fenton processes. *Sci. Total Environ.* **2009**, *407*, 3473–3481. [CrossRef]

49. Huston, P.L.; Pignatello, J.J. Degradation of selected pesticide active ingredients and commercial formulations in water by the photo-assisted Fenton reaction. *Water Res.* **1999**, *33*, 1238–1246. [CrossRef]

50. Monteagudo, J.M.; Duran, A.; Lopez-Almodovar, C. Homogeneous ferrioxalate assisted solar photo-Fenton degradation of Orange II aqueous solutions. *Appl. Catal. B* **2008**, *83*, 46–55. [CrossRef]

51. Maezono, T.; Tokumura, M.; Sekine, M.; Kawase, Y. Hydroxyl radical concentration profile in photo-Fenton oxidation process: Generation and consumption of hydroxyl radicals during the discoloration of azo-dye Orange II. *Chemosphere* **2011**, *82*, 1422–1430. [CrossRef]

52. Alalm, M.G.; Tawfik, A.; Ookawara, S. Degradation of four pharmaceuticals by solar photo-Fenton process: Kinetics and costs estimation. *J. Environ. Chem. Eng.* **2015**, *3*, 46–51. [CrossRef]

53. Dehghani, M.; Shahsavani, E.; Farzadkia, M.; Reza, S.M. Optimizing photo-Fenton like process for the removal of diesel fuel from the aqueous phase. *J. Environ. Health Sci. Eng.* **2014**, *12*, 1–7. [CrossRef] [PubMed]

54. Epold, I.; Dulova, N. Oxidative degradation of levofloxacin in aqueous solution by $S_2O_8^{2-}$/Fe^{2+}, $S_2O_8^{2-}$/H_2O_2 and $S_2O_8^{2-}$/OH^- processes: A comparative study. *J. Environ. Chem. Eng.* **2015**, *3*, 1207–1214. [CrossRef]

55. María, C.Y.; Díaz, L.; Fernández, J. Catalytic activity of the $SO_4^{\bullet-}$ radical for photodegradation of the azo dye Cibacron Brilliant Yellow 3 and 3,4-dichlorophenol: Optimization by application of response surface methodology. *J. Photochem. Photobiol. A Chem.* **2010**, *215*, 90–95.

56. Chia-Chang, L.; Li-Ting, L.; Ling-Jung, H. Performance of UV/$S_2O_8^{2-}$ process in degrading polyvinyl alcohol in aqueous solutions. *J. Photochem. Photobiol. A Chem.* **2013**, *252*, 1–7.

57. Guan, Y.H.; Jun, M.; Li, X.C.; Fang, J.Y.; Chen, L.W. Influence of pH on the Formation of Sulfate and Hydroxyl Radicals in the UV/Peroxymonosulfate System. *Environ. Sci. Technol.* **2011**, *45*, 9308–9314. [CrossRef] [PubMed]

58. Furman, O.S.; Teel, A.L.; Watts, R.J. Mechanism of base activation of persulfate. *Environ. Sci. Technol.* **2010**, *44*, 6423–6428. [CrossRef]

59. Liu, Y.; He, X.; Fu, Y.; Dionysiou, D.D. Kinetics and mechanism investigation on the destruction of oxytetracycline by UV-254 nm activation of persulfate. *J. Hazard. Mater.* **2016**, *305*, 229–239. [CrossRef]

60. Lin, Y.T.; Liang, C.; Chen, J.H. Feasibility study of ultraviolet activated persulfate oxidation of phenol. *Chemosphere* **2011**, *82*, 1168–1172. [CrossRef]

61. Lee, Y.C.; Lo, S.L.; Kuo, J.; Lin, Y.L. Persulfate oxidation of perfluorooctanoic acid under the temperatures of 20–40 °C. *Chem. Eng. J.* **2012**, *198–199*, 27–30. [CrossRef]

62. Lu, X.; Shao, Y.; Gao, N.; Chen, J.; Zhang, Y.; Xiang, H.; Guo, Y. Degradation of diclofenac by UV-activated persulfate process: Kinetic studies, degradation pathways and toxicity assessments. *Ecotoxicol. Environ. Saf.* **2017**, *141*, 139–147. [CrossRef] [PubMed]

63. Saien, J.; Osali, M.; Soleymani, A.R. UV/persulfate and UV/hydrogen peroxide processes for the treatment of salicylic acid: Effect of operating parameters, kinetic, and energy consumption. *Desalin. Water Treat.* **2014**, *56*, 3087–3095. [CrossRef]

64. Liang, C.; Wang, Z.S.; Bruell, C.J. Influence of pH on persulfate oxidation of TCE at ambient temperatures. *Chemosphere* **2007**, *66*, 106–113. [CrossRef] [PubMed]

65. Yuan, R.; Wang, Z.; Hu, Y.; Wang, B.; Gao, S. Probing the radical chemistry in UV/persulfate-based saline wastewater treatment: Kinetics modeling and by products identification. *Chemosphere* **2014**, *109*, 106–112. [CrossRef] [PubMed]

66. Rathi, A.; Rajor, H.K.; Sharma, R.K. Photodegradation of Direct Yellow-12 Using UV/H_2O_2/Fe^{2+}. *J. Hazard. Mater.* **2003**, *102*, 231–241. [CrossRef]

67. Ravichandran, L.; Selvam, K.; Swaminathan, M. Photo-Fenton Defluoridation of Pentafluorobenzoic Acid with UV-C Light. *J. Photochem. Photobiol. A Chem.* **2007**, *188*, 392–398. [CrossRef]

68. Wang, S.; Zhou, N.; Wu, S.; Zhang, Q.; Yang, Z. Modeling the oxidation kinetics of sono-activated persulfate's process on the degradation of humic acid. *Ultrason. Sonochem.* **2015**, *23*, 128–134. [CrossRef]

69. Li, B.; Li, L.; Lin, K.; Zhang, W.; Lu, S.; Luo, Q. Removal of 1,1,1-trichloroethane from aqueous solution by a sono-activated persulfate process. *Ultrason. Sonochem.* **2013**, *20*, 855–863. [CrossRef]

70. Chu, W.; Li, D.; Gao, N.; Templeton, M.R.; Tan, C.; Gao, Y. The control of emerging haloacetamide DBP precursors with UV/Persulfate treatment. *Water Res.* **2015**, *72*, 340–348. [CrossRef]

71. Pengchao, X.; Jun, M.; Wei, L.; Jing, Z.; Siyang, Y.; Xuchun, L.; Wiesner, R.M.; Jingyun, F. Removal of 2-MIB and geosmin using UV/Persulfate: Contributions of hydroxyl and sulfate radicals. *Water Res.* **2015**, *69*, 223–233.

72. Hori, H.; Yamamoto, A.; Hayakawa, E.; Taniyasu, S.; Yamashita, N.; Kutsuna, S.; Kiatagawa, H.; Arakawa, R. Efficient decomposition of environmentally persistent perfluorocarboxylic acids by use of persulfate as a photochemical oxidant. *Environ. Sci. Technol.* **2005**, *39*, 2383–2388. [CrossRef]

73. Gulsen, H.; Turan, M. Treatment of sanitary landfill leachate using a combined anaerobic fluidized bed reactor and Fenton's oxidation. *Environ. Eng. Sci.* **2004**, *21*, 627–636. [CrossRef]

74. Zhang, H.; Choi, H.J.; Huang, C.P. Optimization of Fenton process for the treatment of landfill leachate. *J. Hazard. Mater. B* **2005**, *125*, 166–174. [CrossRef] [PubMed]

75. Asgari, G.; Mohammadi, A.S.; Poormohammadi, A.; Ahmadian, M. Removal of cyanide from aqueous solution by adsorption onto bone charcoal, Fresenius. *Environ. Bull.* **2006**, *23*, 720–727.

76. Muruganandham, M.; Swaminathan, M. TiO_2–UV photocatalytic oxidation of Reactive Yellow 14: Effect of operational parameters. *J. Hazard. Mater.* **2006**, *135*, 78–86. [CrossRef] [PubMed]

77. Shu, H.Y.; Huang, S.W.; Tsai, M.K. Comparative study of acid blue 113 wastewater degradation and mineralization by UV/persulfate and UV/Oxone processes. *Desalin. Water Treat.* **2016**, *57*, 29517–29530. [CrossRef]

78. Rivas, F.J.; Beltrán, F.; Gimeno, O.; Carvalho, F. Fenton-like oxidation of landfill leachate. *J. Environ. Sci. Health A* **2003**, *38*, 371–379. [CrossRef]